Vector-valued intensity measures for pulse-like near-fault ground motions

Jack W. Baker*, C. Allin Cornell

Department of Civil and Environmental Engineering, Stanford University, Stanford, USA

Abstract

A vector-valued intensity measure (IM) is shown to account for the effects of pulse-like near-fault ground motions. This class of ground motions, which are indicated by the presence of a velocity pulse, can cause large responses in structures and their effects are not well described by traditional intensity measures such as spectral acceleration at the structure's first-mode period, $Sa(T_1)$. It is seen that the period of the velocity pulse is an important parameter affecting structural response, and a vector intensity measure which combines $Sa(T_1)$ with a measure of spectral shape is much more effective at accounting for the effects of this pulse period. By performing probabilistic seismic hazard analysis for this IM and combining the results with predictions of structural response as a function of the IM, it is possible to account for near-fault effects when assessing the reliability of structures located at sites where pulse-like ground motions may occur.
© 2007 Elsevier Ltd. All rights reserved.

Keywords: Ground motions; Near-fault; Intensity measure; Record selection; Spectral shape

1. Introduction

Pulse-like near-fault ground motions resulting from directivity effects are a special class of ground motions that are particularly challenging to characterize for seismic reliability assessment. These motions are characterized by a 'pulse' in the velocity time history of the motion, in the direction perpendicular to the fault rupture (e.g., Fig. 1), and generally occur at locations near the fault where the earthquake rupture has propagated towards the site. (Note that this definition includes only records with directivity and excludes records with fling effects). It is important to understand the effects of these ground motions on structures, because they have been observed to cause structural damage in the past. It has been observed that these motions have, on average, larger elastic spectral acceleration values at moderate to long periods. This has been addressed by modifying ground motion prediction ('attenuation') models to have larger median predicted intensities at locations where directivity effects are expected [1]. Additionally, these motions tend to cause severe response of nonlinear multi-degree-of-freedom structures to an extent not entirely accounted for by measuring
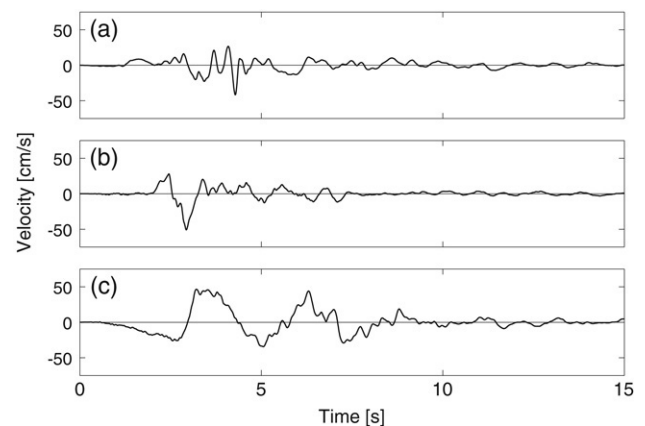

Fig. 1. Velocity time histories for the three pulse-like ground motions, after scaling each so that Sa (0.9 s) = 0.5*g*. (a) Record 1: Morgan Hill, Anderson Dam; T_p = 0.45 s, Magnitude = 6.2, Distance = 3 km. (b) Record 2: Kobe, KJMA; T_p = 0.85 s, Magnitude = 6.9, Distance = 1 km. (c) Record 3: Superstition Hills, Parachute Test Site; T_p = 1.9 s, Magnitude = 6.5, Distance = 1 km.

the intensity of the ground motion using spectral acceleration of the elastic first-mode period of a structure, $Sa(T_1)$ [2,3].

A ground motion intensity measure (IM) that is better able to predict the effects of pulse-like ground motions, as well as a method to calculate seismic hazard for that IM, could facilitate

---

* Corresponding address: Department of Civil and Environmental Engineering, Terman Engineering Center #234, Stanford, CA 94305-4020, USA. Tel.: +1 650 725 2573; fax: +1 650 723 7514.

E-mail address: bakerjw@stanford.edu (J.W. Baker).

better assessment of the reliability of structures subjected to these ground motions. Here an improved vector-valued measure of ground motion intensity is considered for structural response prediction, with attention also given to computing occurrence rates for this IM using extensions of standard probabilistic seismic hazard analysis.

2. Pulse-like ground motions

Sites located near an earthquake fault rupture may experience ground shaking that includes a velocity 'pulse'. This pulse is most likely to occur in specific site–source geometrical configurations (see, e.g., [1]). Generally, a velocity pulse is likely to occur in the fault-normal direction at sites within 20 to 30 km of a fault where the earthquake rupture is propagating towards the site. Ground motion shaking in the fault-parallel direction is typically less intense. In the discussion that follows, the term 'pulse-like ground motion' is used to refer to fault-normal ground motions with an observed velocity pulse, typically occurring within 20 or 30 km of the fault.

A set of 70 pulse-like ground motions collected by Tothong and Cornell [4] is utilized in this study. This set is an aggregation of records identified in three previous papers [5–7]. All ground motions were recorded on firm soil or rock sites and at least one of the referenced authors has identified a pulse in the velocity time history. By using previously identified ground motions, a set of 'pulse-like' near-fault ground motions can be utilized here while avoiding a discussion of the complex issues relating to source and wave propagation mechanisms causing this type of ground motion.

The processed ground motions come from the Next Generation Attenuation project database (http://peer.berkeley.edu/nga/), and are oriented in the fault-normal direction. An important property of pulse-like ground motions is the period of the velocity pulse, denoted T_p; following Alavi and Krawinkler [3], T_p is measured as the period associated with the maximum of the velocity response spectrum. Forty 'ordinary' ground motions with no velocity pulses are also used for comparison with the pulse-like record set. Record properties are given in Baker and Cornell [8, Table A.3–A.4].

At large periods, pulse-like ground motions tend to cause larger elastic spectral acceleration (Sa) levels than standard ground motion (attenuation) models predict. A model for this effect was proposed by Somerville et al. [1], in the form of a modification to a popular ground motion prediction model [9], with the intention that the correction could be applied to other prediction models as well. This 'wide band' model adjusts a broad range of spectral acceleration values at periods greater than 0.6 s. Future 'narrow band' models will adjust a smaller range of spectral acceleration values depending upon the period of the velocity pulse, which is related to the magnitude of the earthquake [10]. Regardless of the exact form of the ground motion prediction model, Sa values tend to be larger, at least at longer periods, for ground motions with velocity pulses than for ordinary ground motions with similar magnitudes and distances. But, as will be seen below, these larger Sa values

Table 1
Model parameters for the four generic-frame structures considered in this chapter

Number of stories (N)	Elastic first-mode period (T_1), (s)	Elastic second-mode period, (s)	Ductility capacity (δ_c/δ_y)	Post-capping stiffness coefficient (α_c)	Cyclic deterioration parameters ($\gamma_{s,c,k,a}$)
3	0.3	0.10	4	−0.5	50
9	0.9	0.34	4	−0.5	50
6	1.2	0.47	4	−0.5	50
9	1.8	0.71	4	−0.5	50

do not completely account for the larger structural responses observed from these records.

3. Structural response to pulse-like ground motions

To quantify the effect of pulse-like ground motions, four multi-degree-of-freedom nonlinear structures designed by Ibarra and Krawinkler [11] are used for evaluation. The structures are generic single-bay frames, with properties chosen to be representative of typical structures. Their important properties are given in Table 1. To summarize results from these various structures, structural response data is reported for ground motions scaled such that the records' $Sa(T_1)$ level in units of g is a specified multiple of the structure's base shear coefficient γ, where γ = yield base shear/weight [12]. The ratio $Sa(T_1)/\gamma$ is analogous to an R-factor in present building codes, if there was no overstrength in the structure. Using this normalized ground motion intensity measure, all four structures will yield at $Sa(T_1)/\gamma$ factors of approximately one (recognizing that higher-mode response may or may not induce yielding at this $Sa(T_1)/\gamma$ level). Increasing $Sa(T_1)/\gamma$ levels will correspond to increasing levels of nonlinearity in the structures.

The ground motions were all scaled to several levels of $Sa(T_1)/\gamma$ for each structure, and then input into the structure in order to compute structural response. The response parameter considered here is the maximum interstory drift ratio observed in any story, as it is a good indicator of the ability of a structure to resist $P-\Delta$ instability and collapse, as well as maximum rotation demands on beams, columns and connections [13]. Peak interstory drift ratios in these structures are known to be significantly affected by second-mode response (Helmut Krawinkler personal communication 2005); this feature of the structures will help demonstrate the ability of a vector IM to account for higher-mode response when the structure is linear, but the effect of higher-mode response is likely less significant for most typical structures with comparable numbers of stories and/or comparable first-mode periods.

An important parameter of pulse-like motions that affects structural response is the period of the velocity pulse with respect to the modal periods of the structure [3,14–18]. In Fig. 2, calculated maximum interstory drift ratios for the nine-story structure with a period of 0.9 s are plotted versus the ground motions' pulse periods. To illustrate local variations in
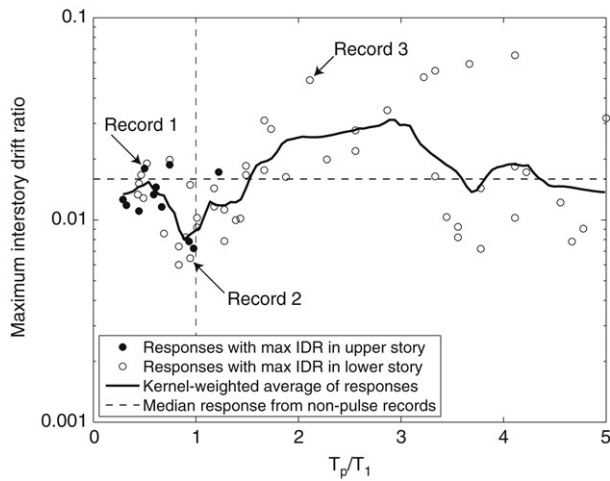
Fig. 2. Maximum interstory drift ratio from pulse-like records versus T_p/T_1 for the generic frame with 9 stories and a first-mode period of 0.9 s at an $Sa(T_1)/\gamma$ level of 4. The records labeled 1, 2 and 3 correspond to the records identified in Fig. 1.
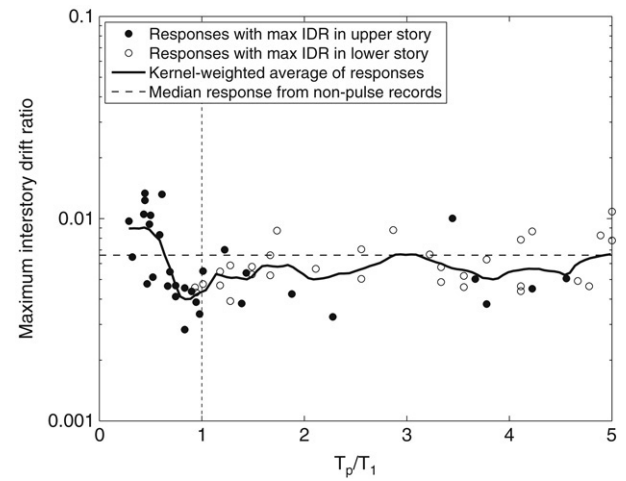

Fig. 4. Maximum interstory drift ratios from pulse-like records versus T_p/T_1 for the generic frame with 9 stories and a first-mode period of 0.9 s, at an $Sa(T_1)/\gamma$ level of 2.
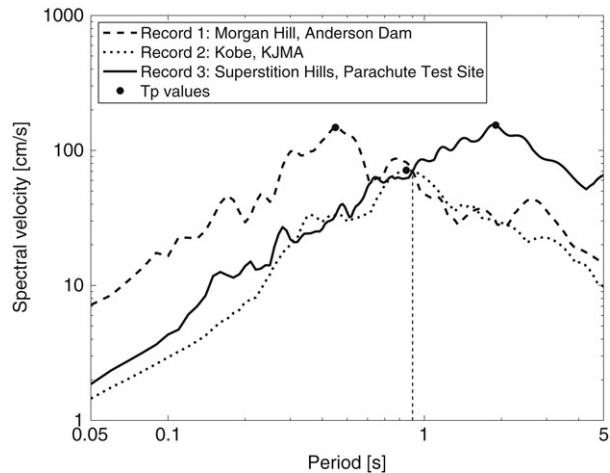

Fig. 3. Velocity spectra of the records from Fig. 1, after scaling each record so that $Sv(0.9\ s) = 70$ cm/s or, equivalently, $Sa(0.9\ s) = 0.5g$.

the data, a local average is plotted (using the Nadaraya–Watson kernel-weighted average, with a tri-cube weight function and an adaptive window that includes the 10 nearest neighbors [19]). Results are shown for ground motions scaled such that $Sa(T_1)/\gamma = 4$. Three records are highlighted in Fig. 2, and their associated (pseudo)velocity spectra are shown in Fig. 3. Velocity spectra, $Sv(T) = Sa(T) \cdot (T/2\pi)$, are plotted instead of (pseudo)acceleration spectra because the two differ only by a constant and periods of near-fault pulses are clearer in the velocity spectrum. Use of spectral velocity values as IM parameters would give the same results as the spectral acceleration values considered here, but spectral acceleration values are used for consistency with standard ground motion prediction models and hazard maps.

Some of the trends in Fig. 2 are observed systematically for a range of structures and $Sa(T_1)/\gamma$ factors. For T_p/T_1 values near 2 or 3, the response is relatively large compared to the response from records with shorter-period pulses. This is because $Sa(T_1)$ only measures the intensity of the ground

motion at T_1. As the structure behaves nonlinearly and its effective period lengthens, it is greatly affected by velocity pulses at longer periods (see, e.g., the response spectrum of Record 3 in Fig. 3). Conversely, the minimum responses are associated with records having T_p/T_1 values of approximately 1. In this case a record's $Sa(T_1)$ value will be large because of the energy from the pulse with a period of approximately T_1, implying that the record is intense as measured by $Sa(T_1)$. But as the structure begins to behave nonlinearly, its period lengthens into a range where there is comparatively lesser energy (see, e.g., the response spectrum of Record 2 in Fig. 3). Finally, for T_p/T_1 values near 0.3, the pulse excites higher modes of the structure, although the IM $Sa(T_1)$ cannot detect it. As mentioned previously, the structures considered here are particularly sensitive to second-mode excitation, so records with T_p/T_1 values in this range can also cause large responses. The effect of short-period pulses can also be confirmed by noting that for records with $T_p/T_1 < 1$ the maximum responses are often observed in the upper stories (as shown in Fig. 2), indicating that the higher modes of vibration are contributing significantly to these responses. Conversely, for records with T_p/T_1 values greater than one, maximum responses nearly always occur in the lower stories, indicating that first-mode response is controlling peak displacements. The effect of pulses on higher modes is also seen in Fig. 4, which is identical to Fig. 2 except that the records have been scaled to an $Sa(T_1)/\gamma$ factor of 2. Records with T_p/T_1 values larger than one do not affect the structure significantly at this $Sa(T_1)/\gamma$ level associated with lower nonlinearity. Records with T_p/T_1 values near the second-mode period of the structure, however, do cause larger responses, and peak responses always occur in the upper stories of the structure, indicating the effect of higher modes.

Note that although modal analysis concepts are theoretically correct only for linear structures, they have been observed empirically to provide useful insight into the behavior of moderately nonlinear structures (e.g., [20]). Nonlinear time history analysis, as opposed to modal analysis, was used to compute all structural response results shown here, and

modal concepts are only mentioned to the extent that they are consistent with observed results.

If the responses from records scaled to a given IM are insensitive to other properties of the ground motion, then the ground motion intensity measure is termed 'sufficient' [21]. As seen in Figs. 2 and 4, $Sa(T_1)$ is not sufficient with respect to T_p, so the response estimated from pulse-like records at a given $Sa(T_1)$ level will depend upon the particular records used for analysis. This is a concern for estimating response from pulse-like records, because it is not obvious which records best represent potential future ground motions at the site (i.e., which records will give the 'correct' answer). If an improved intensity measure can be shown to be sufficient with respect to T_p, then response estimates can be obtained that are only a function of the target ground motion intensity, which can be computed using ground motion hazard analysis, and not dependent upon the specific records used.

Two subsets of the pulse-like records are also compared with the ordinary ground motions, to further study the effect of T_p/T_1. The records with $T_p/T_1 > 2$ are separated and labeled 'aggressive' pulse-like ground motions, and the records with $0.5 < T_p/T_1 < 1.5$ are separated and labeled 'benign' pulse-like ground motions. Although a ground motion with T_p/T_1 close to one will likely have a large $Sa(T_1)$ value, it is called a benign motion because, *given* $Sa(T_1)$, it will have relatively small spectral values at other periods and thus tend to cause smaller response, as illustrated by Record 2 in Fig. 2. These two subsets are compared to the complete set of pulse-like ground motions and to the ordinary ground motions with no velocity pulse. In Fig. 5 the median maximum interstory drift ratio is plotted versus $Sa(T_1)/\gamma$ for all four groups of ground motions. In Fig. 6, the probability of collapse is plotted for the same four groups of ground motions, where collapse of these structures is indicated by large interstory drifts that cause non-convergence of the analysis program. The aggressive pulse-like records have the largest median responses for $Sa(T_1)/\gamma$ factors greater than 2, and greater probabilities of collapse for $Sa(T_1)/\gamma$ factors greater than 6. The benign pulse-like ground motions have the smallest median responses and the smallest probabilities of collapse at all $Sa(T_1)/\gamma$ factor levels. The median probabilities of collapse are nearly equal for the ordinary ground motions and the set of all pulse-like ground motions. But the pulse-like ground motion collapse distribution has heavier tails, due to the presence of the benign and aggressive ground motions, which cause greater record-to-record variability than the ordinary ground motions. These results indicate that some pulse-like ground motions cause relatively severe responses in a structure and some do not. If an improved intensity measure can better distinguish between the benign and aggressive records, then the sufficiency problems of $Sa(T_1)$ might be addressed and IM-based structural reliability assessments would be feasible even when pulse-like ground motions are considered [21].

4. A vector-valued IM with $Sa(T_1)$ and $R_{T1,T2}$

A vector-valued IM based on spectral acceleration values at two periods has been found to be a useful predictor for ordinary
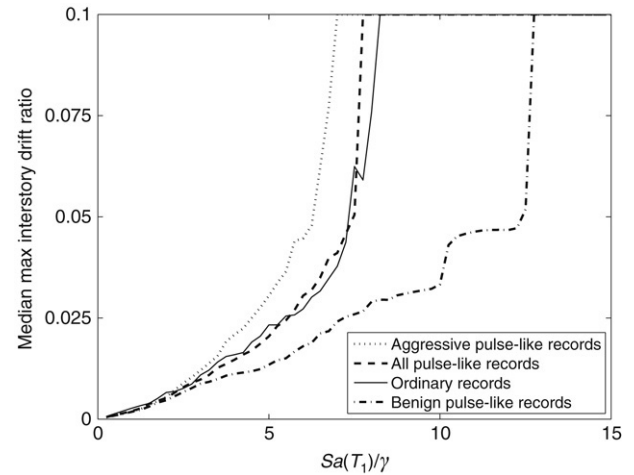

Fig. 5. Median maximum interstory drift ratio versus normalized spectral acceleration $(Sa(T_1)/\gamma)$ for the generic frame with 9 stories and a first-mode period of 0.9 s.
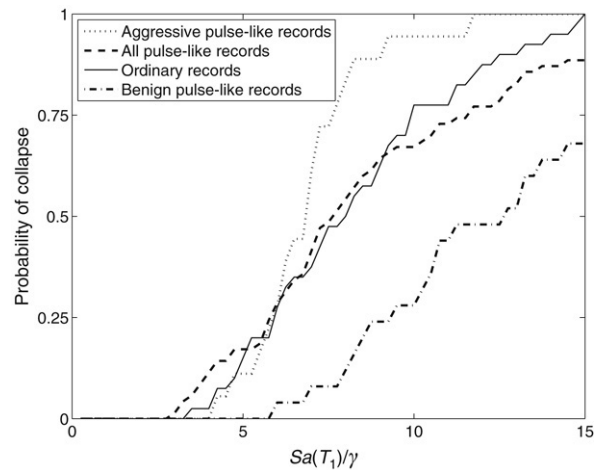

Fig. 6. Counted probabilities of collapse versus normalized spectral acceleration $(Sa(T_1)/\gamma)$ for the generic frame with 9 stories and a first-mode period of 0.9 s.

ground motions [22–24]. The IM consists of the parameters $Sa(T_1)$ and $R_{T1,T2} = Sa(T_2)/Sa(T_1)$, where T_1 is constrained to equal the first-mode period of the structure and T_2 is chosen to capture important characteristics of the spectrum's shape. Depending upon whether T_2 is smaller or larger than T_1, this intensity measure can provide information about excitation of higher modes or nonlinear response, respectively. In much of the following investigation, T_2 will be specified as twice the elastic first-mode period. This choice of T_2 may be intuitive because it has been seen to be effective for predicting the response of structures subjected to ordinary ground motions [24], and it is also in the period range of particular concern for pulse-like motions, as noted earlier. Consideration will also be given to the choice $T_2 = T_1/3$, in an attempt to account for pulses that affect higher-mode structural response.
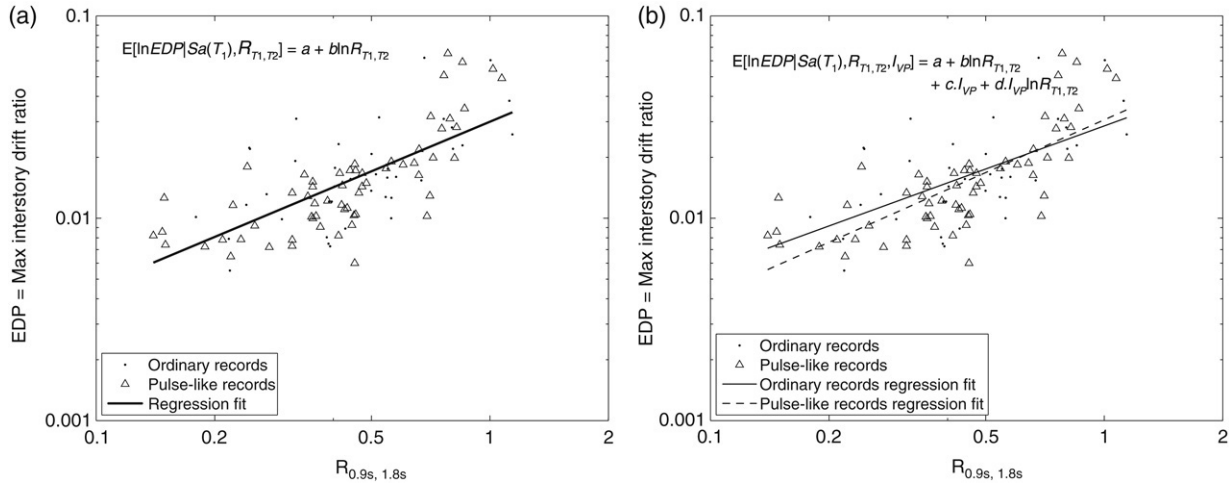
Fig. 7. Prediction of EDP for the generic frame with 9 stories and a first-mode period of 0.9 s, using linear regression on $R_{0.9 \text{ s}, 1.8 \text{ s}}$ with records scaled such that the structure's $Sa(T_1)/\gamma$ level is 4. (a) Estimate of all responses using the same prediction equation. (b) Estimate of responses using separate equations for ordinary and pulse-like ground motions.

4.1. The effect of $R_{T1,T2}$ on pulse-like and ordinary ground motions

The first step in investigating the relationship between $R_{T1,T2}$ and T_p is verifying that $R_{T1,T2}$ predicts structural response in the same way for both ordinary and pulse-like records. One alternative is that ordinary and pulse-like ground motions cause the same mean structural response as a function of $R_{T1,T2}$. Here the structural response parameter, which is termed an Engineering Demand Parameter (EDP) by the Pacific Earthquake Engineering Research Center, is maximum interstory drift ratio. Prediction of response is made using linear regression, after logarithmic transformations, following earlier work with this predictor [22–24]. Based on empirical statistical studies using large sets of structural response data, a reasonable predictive equation for this alternative is

$$E[\ln EDP | Sa(T_1), R_{T1,T2}] = a + b \ln R_{T1,T2} \qquad (1)$$

where a and b are coefficients to be estimated from regression analysis used EDP results from records scaled to a specified level of $Sa(T_1)$. Alternatively, pulse-like and ordinary ground motions may have differing functional relationships between $R_{T1,T2}$ and structural response. This alternative can be expressed using the equation

$$E[\ln EDP | Sa(T_1), R_{T1,T2}, I_{VP}]$$
$$= a + b \ln R_{T1,T2} + c \cdot I_{VP} + d \cdot I_{VP} \ln R_{T1,T2} \qquad (2)$$

where I_{VP} is an indicator variable equal to 1 if the given record has a velocity pulse and equal to 0 otherwise, and c and d are additional regression coefficients. Fitted predictions using these two models are shown in Fig. 7.

A statistical test known as an F test [25] can be used to choose between the two models. The simpler alternative of Eq. (1) (called the null hypothesis) is assumed to be the truth until evidence is found to the contrary. If the prediction errors using the model of Eq. (2) (the alternative hypothesis) are significantly smaller than the errors from Eq.

(1), this is taken as evidence that the more complex model is appropriate. An F statistic is computed by comparing the aggregate prediction errors from the two models, and the p-value associated with the statistic provides the probability that the apparent improvement from the null hypothesis to the alternative hypothesis would be observed, even though (i.e., 'given that') the null hypothesis is actually true. P-values below 0.05 are usually assumed to indicate significant improvement using the more complex model. The p-value associated with Fig. 7 is 0.52, indicating that there is no empirical justification for using the more complex model because it does not improve predictive accuracy. P-values for a range of structures and Sa levels are tabulated in Table 2. If the simple model holds, approximately 5% of p-values will be below 0.05. In Table 2, 7.7% of the tests have p-values below 5%, indicating that the simpler model of Eq. (1) can be used: no distinction need be made between pulse-like and ordinary records when predicting response based on $R_{T1,T2}$. This is important because it suggests that an analyst need not distinguish between pulse-like and ordinary records when predicting response as a function of $Sa(T_1)$ and $R_{T1,T2}$.

4.2. Sufficiency with respect to T_p

To determine whether $R_{T1,T2}$ is able to account for the effect of T_p on structural response, the nine-story structure with a first-mode period of 0.9 s and an $Sa(T_1)/\gamma$ factor of 4 is again considered. The difference between the mean response and individual record responses is plotted versus T_p in Fig. 8(a); this plot uses the same data as Fig. 2, but is normalized with respect to the mean response. Next, prediction based on the vector IM including $R_{T1,T2}$ (with T_2 equal to 1.8 s) is considered; the prediction based on this IM was shown in Fig. 7(a). The residuals from this prediction are plotted in Fig. 8(b), and there is a dramatic reduction in the dependence between T_p and structural response, relative to the predictions based on $Sa(T_1)$ alone. The standard deviation of the residuals is also reduced by

Table 2
P-values from F tests to test the hypothesis that the relationship between $R_{T1,T2}$ and maximum interstory drift ratio is different for pulse records and non-pulse records

(a) $Sa(T_1)/\gamma$ level	Structure				(b) $Sa(T_1)/\gamma$ level	Structure			
	$N = 3$, $T_1 = 0.3$ s	$N = 9$, $T_1 = 0.9$ s	$N = 6$, $T_1 = 1.2$ s	$N = 9$, $T_1 = 1.8$ s		$N = 3$, $T_1 = 0.3$ s	$N = 9$, $T_1 = 0.9$ s	$N = 6$, $T_1 = 1.2$ s	$N = 9$, $T_1 = 1.8$ s
0.5	0.14	0.19	0.08	0.95	0.5	0.20	0.40	0.31	**0.01**
1.0	0.14	0.29	0.07	0.83	1.0	0.20	0.35	0.14	**0.04**
2.0	**0.04**	0.65	0.27	0.91	2.0	0.47	0.28	**0.02**	0.25
3.0	0.13	0.22	0.66	0.21	3.0	0.23	0.06	0.19	0.17
4.0	0.32	0.52	0.30	0.71	4.0	0.50	0.12	0.24	0.90
5.0		0.36	0.90	0.53	5.0		0.41	0.62	0.67
6.0		0.80	0.93		6.0		0.44	0.90	
7.0		0.48			7.0		0.98		

The tests are performed for two choices of T_2: (a) $T_2 = 2T_1$ and (b) $T_2 = T_1/3$. *P*-values are not reported for levels with more than 50% of the records causing collapse.
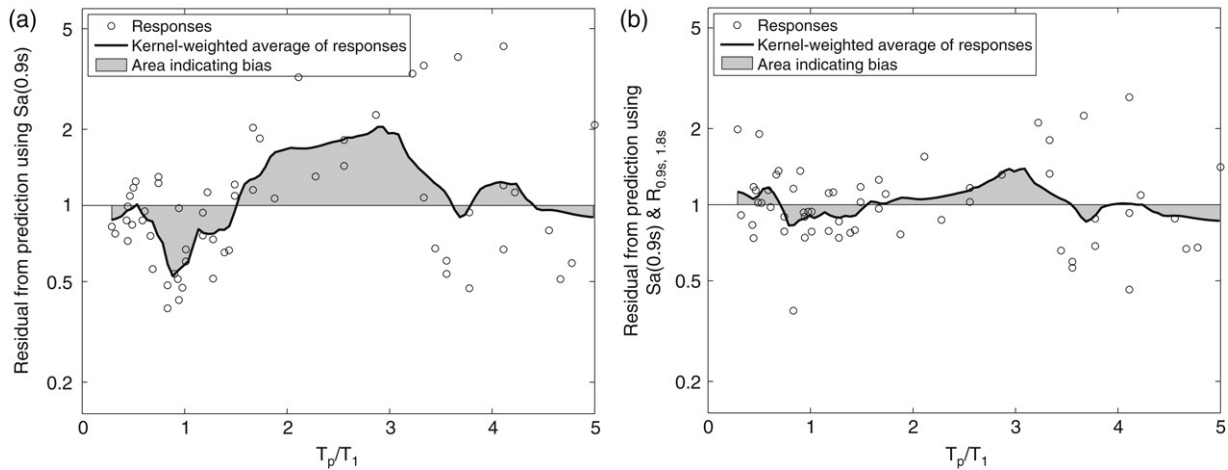

Fig. 8. Residuals from response prediction based on (a) $Sa(T_1)$ only, and (b) both $Sa(T_1)$ and $R_{T1,T2}$, plotted versus T_p/T_1 for the generic frame with 9 stories and a first-mode period of 0.9 s, at an $Sa(T_1)/\gamma$ level of 4.

34%, so reductions have been made in variance as well as bias with respect to pulse-like records.

The effectiveness of $R_{T1,T2}$ in this case can be explained by examining the plot of T_p versus $R_{T1,T2}$ in Fig. 9. The shapes of the average trends in Figs. 9 and 8(a) are very similar, indicating that $R_{T1,T2}$ and T_p are related. When $T_p/T_1 \cong 1$, $R_{T1,T2}$ tends to be small because $Sa(T_2)$ is lower than the peak caused by the pulse. But when $T_p/T_1 \cong 2$, $R_{T1,T2}$ tends to be large because $Sa(T_2)$ is on a spectral peak caused by the pulse.

Other periods besides $T_2 = 2T_1$ may also account for the effect of velocity pulses. To measure the effectiveness of various T_2 choices, a statistic was designed to measure the reduction in potential bias. The total area between the kernel-weighted average line and the zero residual line is taken as a proxy for the effect of T_p that is unaccounted for by the IM, as illustrated in Fig. 8; the total area is summed, so positively and negatively biased regions are not offsetting. The shaded area is reduced by 65% from Fig. 8(a) to (b). This fractional reduction depends upon the T_2 value chosen for $R_{T1,T2}$. In Fig. 10, the fractional reduction is plotted versus T_2 for all four structures;

the results for the structure studied in Fig. 8 are plotted with a heavy line for emphasis. The optimal T_2 in this case is exactly $2T_1$, but T_2 values between $1.7T_1$ and $2.4T_1$ all provide at least 75% of the improvement attained using the optimal T_2. The value $T_2 = 2T_1$ is seen to be nearly optimal T_2 for all four of the structures considered. Similar tests at other $Sa(T_1)/\gamma$ levels indicate that $T_2 = 2T_1$ is an effective choice for a wide range of ground motion intensities associated with moderate to high nonlinearity.

Higher-mode effects were seen in Fig. 4 to be more important than nonlinear effects at low $Sa(T_1)/\gamma$ levels. For this reason, $T_2 = T_1/3$ was selected as the second period for tests at an $Sa(T_1)/\gamma$ level of 2. The residuals from prediction based on $Sa(T_1)$ alone and based on $Sa(T_1)$ and $R_{T1,T2}$ are shown in Fig. 11. Again, $R_{T1,T2}$ substantially accounts for the effect of T_p on structural response, especially for the short-period records which excite higher modes. Plots similar to Fig. 10 at low levels of nonlinearity indicate that T_2 values less than T_1 produce a reduction in bias, while longer periods are not effective. This situation is likely of less engineering interest,
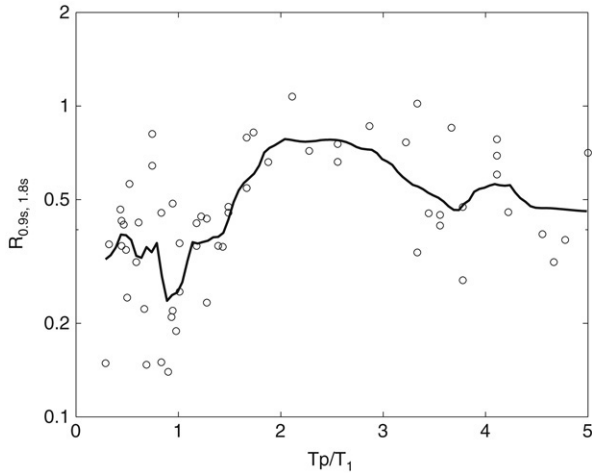
Fig. 9. T_p versus $R_{T1,T2}$ for the pulse-like ground motions, with $T_1 = 0.9$ s.
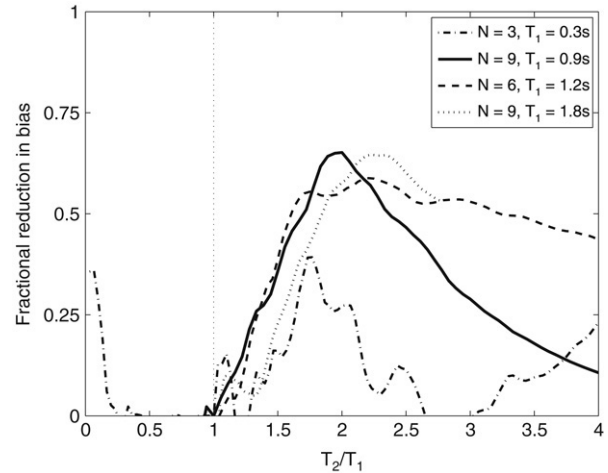

Fig. 10. Percentage reduction in the proposed bias statistic versus the T_2 value used in $R_{T1,T2}$. Results are shown for all four structures at an $Sa(T_1)/\gamma$ level of 4.

however, than the moderate to high nonlinearity cases where T_2 value greater than the first-mode period of structure are most effective.

5. Alternative intensity measures

Other intensity measures have been proposed recently for improved prediction of structural response, and their potential effectiveness at accounting for pulse-like ground motions is addressed briefly here. A vector IM that has been the focus of recent research consists of $Sa(T_1)$ and the ground motion parameter ε [26]. Epsilon is a measure of the difference between a record's spectral acceleration value at a given period and the mean value of a predictive model; here the near-fault predictive model of Somerville et al. [1] was used to compute the epsilon values. This IM has been observed to effectively account for spectral shape in ordinary ground motions, but when the above tests were repeated using ε, it was seen to be ineffective at accounting for the effect of velocity pulses in the ground motions [8]. This was expected, however, because ε measures peaks and valleys in the response spectrum at T_1,

and the presence of velocity pulses at other periods does not significantly affect these peaks and valleys.

Luco and Cornell [21] have developed an intensity measure based on inelastic spectral response values, and observed that it is effective at predicting the response of structures subjected to pulse-like records. Comparison of the IM proposed here to the IM proposed by Luco and Cornell is a topic of current research. For both of these IMs, challenges remain for characterizing the ground motion hazard.

6. PSHA for pulse-like ground motions

To make full use of predictions based on $Sa(T_1)$ and $R_{T1,T2}$, it is necessary to compute the rates of joint occurrence of $Sa(T_1)$ and $R_{T1,T2}$ values at the site, which can then be coupled with structural response predictions to estimate seismic reliability. Bazzurro and Cornell [27] have described this procedure, termed Vector-valued Probabilistic Seismic Hazard Analysis (VPSHA), for sites subjected to ordinary ground motions, but it requires some modification for use at sites with
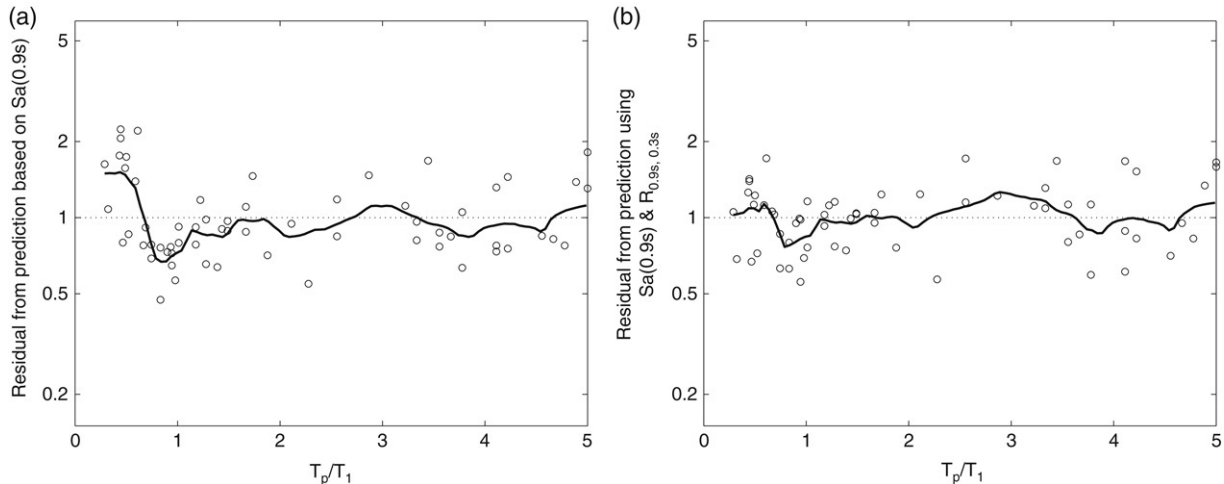

Fig. 11. Residuals from response prediction based on (a) $Sa(T_1)$ only, and (b) both $Sa(T_1)$ and $R_{T1,T2}$, plotted versus T_p/T_1 for the generic frame with 9 stories and a first-mode period of 0.9 s, at an $Sa(T_1)/\gamma$ level of 2. $T_2 = 0.3$ s for this plot.

pulse-like ground motions. Two approaches for performing VPSHA are briefly described here.

The simplest approach to performing VPSHA for pulse-like motions is based on the method used by Bazzurro and Cornell [27]. They represent the distribution of $\ln R_{T1,T2}$ and $\ln Sa(T_1)$ for a given earthquake event as a joint normal random variable, where the conditional dependence between the two is fully defined by a correlation coefficient. The approach can be modified by adjusting the means, variances and correlation coefficients of the ground motion predictions to account for the possible occurrence of pulse-like motions. This can be implemented using existing attenuation models for pulse-like ground motions. At present, one prediction model exists for pulse-like ground motions [1], and it has been used to perform PSHA for scalar IMs while accounting for pulse-like ground motions [28]. For VPSHA, correlation coefficients are also needed for spectral acceleration values at differing periods, and empirical observations of the needed coefficients have been reported [8, Appendix C].

This procedure is straightforward to implement, but some of the model assumptions may be questionable for near-fault environments. Response spectral values for pulse-like ground motions are dependent upon the period of the pulse, but this is not captured in current ground motion predictions. Further, the occurrence of a velocity pulse is not certain even at source-to-site geometries where a pulse might be anticipated. If the occurrence of a pulse is a random event and the period of the pulse is a random variable, then the resulting $Sa(T_1)$ value may not be lognormally distributed, as is the case for ordinary ground motions [29]. The distribution may instead be bimodal, with one peak representing records having $T_p \cong T_1$, and another peak associated with the other records. For the same reason, the distribution of $Sa(T_1)$ and $R_{T1,T2}$ might not be jointly lognormal.

To address these shortcomings, Tothong et al. [30] propose an alternative approach to incorporate pulse-like ground motions in PSHA. In addition to accounting for random magnitudes and distances, the model explicitly accounts for the fact that velocity pulses are not certain to occur even at sites where they are likely. It also accounts for random pulse periods, and the spectral shapes of pulse-like ground motions of the type observed in Fig. 3. That is, the occurrence of a pulse and its period are treated as explicit random variables so that the ground motion prediction can be made as a function of this information. In the model by Somerville et al. [1], ground motions of all types were included when the predictive equation was developed, so the prediction is necessarily less precise. To implement the alternative approach, a new prediction is needed for the probability of occurrence of a velocity pulse for a given magnitude, distance and source–site geometry. The required distribution of pulse period as a function of magnitude has been provided by several researchers [6,7,10]. Also needed is a 'narrow band' near-fault ground motion prediction model that accounts explicitly for the period of the velocity pulse and provides spectral response predictions that are higher near the pulse period than they are elsewhere [10]. This approach allows

for a more explicit representation of the effect of pulse-like ground motions when computing ground motion hazard.

7. Coupling response predictions with PSHA results

If structural response is dependent only on the intensity measure parameters, and is conditionally independent of other ground motion parameters (such as magnitude, distance and pulse period), then the seismic reliability of a structure can be computed by combining PSHA results with predictions of structural response as a function of the IM parameters [31]. These results are obtained using a simple integration which combines the rates of occurrence of various levels of ground motion intensity (i.e., the ground motion hazard), with the distribution of structural response values observed at that level (e.g., [26]). This approach for computing 'structural response hazard' is sometimes referred to as Probabilistic Seismic Demand Analysis (PSDA). The approach is problematic, however, in near-fault environments when $Sa(T_1)$ is used as the IM, as discussed earlier. But when the IM consists of both $Sa(T_1)$ and $R_{T1,T2}$, the effects of velocity pulses are more fully accounted for. This suggests that seismic reliability can be computed with this approach, and the estimates will be insensitive to the ground motions used for analysis (i.e., the presence and periods of velocity pulses in the ground motions).

To verify this insensitivity, PSDA is performed for the same nine-story example structure. The ground motion hazard comes from a site near Los Angeles, California. Ground motion hazard is computed for two intensity measures: Sa (0.9 s), and a vector consisting of Sa (0.9 s) and $R_{0.9\,s,1.8\,s}$. The site is not expected to experience pulse-like ground motions, but the calculation still provides a useful verification that the vector IM proposed here can desensitize PSDA results to the presence of velocity pulses. To accurately perform this assessment at a site where pulse-like ground motions may potentially occur, standard ground motion hazard analysis must be revised, as described above.

The procedure is performed using the four sets of ordinary and near-fault ground motions used earlier, to determine whether the calculated result depends upon the ground motions used. As was seen in Figs. 5 and 6, the four sets of ground motions cause different levels of response in the structure for a given $Sa(0.9\ s)$ level, so the structural response hazard curves computed using $Sa(0.9\ s)$ will vary depending upon which of these ground motion sets are used. As seen in Fig. 12(a), the benign pulse-like records, which were observed to cause smaller responses at a given $Sa(0.9\ s)$ level, result in lower estimates of mean rates of exceeding large maximum interstory drift ratios. Similarly, the aggressive pulse-like records result in higher estimated mean rates of exceedance. However, when the vector IM consisting of $Sa(0.9\ s)$ and $R_{0.9\,s,1.8\,s}$ is used, the variations in estimated structural response hazard are reduced, as seen in Fig. 12(b). When $R_{0.9\,s,1.8\,s}$ is incorporated in the IM, the difference in exceedance rates of 0.1 max interstory drift ratio obtained using the benign and aggressive record sets is reduced by 60%. Similar results are also observed for the other example structures, indicating that the use of the vector IM
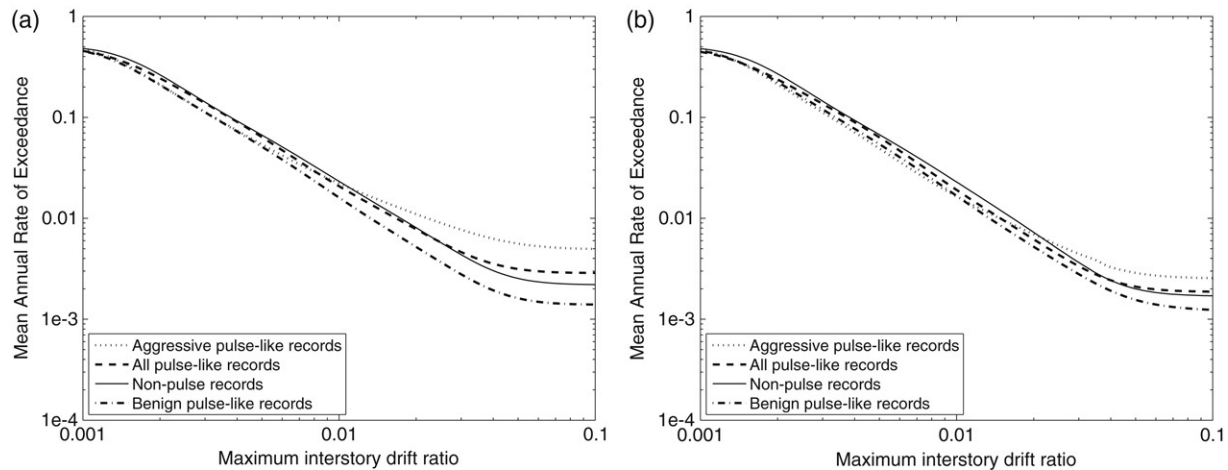
Fig. 12. Drift hazard curves using the four considered record sets. (a) Curves computed using the scalar IM $Sa(0.9 \text{ s})$. (b) Curves computed using the vector IM consisting of $Sa(0.9 \text{ s})$ and $R_{0.9 \text{ s}, 1.8 \text{ s}}$.

consisting of $Sa(T_1)$ and $R_{T1,T2}$ accounts substantially for the effects of velocity pulses in ground motions. This suggests that the PSDA approach may be valid in near-fault environments if the proposed vector IM is used.

8. Conclusions

A vector-valued intensity measure consisting of $Sa(T_1)$ and a measure of spectral shape has been considered for predicting the effects of pulse-like ground motions. Pulse-like ground motions (near-fault ground motions in the fault-normal direction which exhibit a velocity pulse due to directivity effects) are of particular concern to engineers because of their potential to cause large levels of structural response. Further, their effects are not well predicted by traditional measures of ground motion intensity such as elastic spectral acceleration.

The considered intensity measure consists of spectral acceleration at the structure's first-mode period, $Sa(T_1)$, along with a parameter $R_{T1,T2} = Sa(T_2)/Sa(T_1)$ that describes the shape of the response spectrum. This IM has previously been found to efficiently predict maximum interstory drift ratios from ordinary ground motions, especially given wise choice of T_2. Here it was also shown to be effective at predicting maximum interstory drift ratios resulting from pulse-like ground motions. There was no statistically significant difference in maximum interstory drift ratios between ordinary and pulse-like records after the effects of $Sa(T_1)$ and $R_{T1,T2}$ were accounted for, given a reasonable choice of T_2. Further, $Sa(T_1)$ and $R_{T1,T2}$ effectively account for the effect of pulse periods on the structure's resulting maximum interstory drift ratio. For the structures considered here, a choice of T_2 equal to twice the first-mode period of the structure was seen to be effective in the important situation where a ground motion causes moderate to severe nonlinearity in the structure.

In addition to predicting response given $Sa(T_1)$ and $R_{T1,T2}$, ground motion hazard must be computed for this intensity measure in order to assess the seismic reliability of a given structure. To illustrate the usefulness of the vector IM, a ground motion hazard result was computed at a site that is not expected to experience directivity effects. When a ground motion hazard

curve was combined with structural response results to compute annual rates of exceeding various structural response levels using the vector IM, the results were similar whether pulse-like or ordinary ground motions were used. This suggests that when using the vector IM, it is less important to carefully identify representative pulse-like records as is sometimes done today [32]. This is similar to approaches used currently at non-near-fault sites, where ground motion hazard analysis is used to quantify the demands upon the structure in terms of response spectral values, and it is less important that the ground motions used in dynamic analysis be exactly representative of some expected earthquake event. The example ground motion hazard analysis used for illustration of the approach did not account for near-fault effects, but the conclusions will also apply once near-fault ground motion hazard analysis is implemented. Methods for computing near-fault ground motion hazard were briefly discussed, and are a topic of active research.

Maximum interstory drift ratio was the only structural response parameter considered here, but Alavi and Krawinkler [3] observed that pulse-like ground motions can cause different distributions of interstory drift ratios over the height of the structure. Further work is needed to test the robustness of vector IMs for predicting this and other structural response quantities of interest.

Acknowledgements

References

[1] Somerville PG, Smith NF, Graves RW, Abrahamson NA. Modification of empirical strong ground motion attenuation relations to include the amplitude and duration effects of rupture directivity. Seismological Research Letters 1997;68(1):199–222.

[2] Baez J, Miranda E. Amplification factors to estimate inelastic displacement demands for the design of structures in the near field. In: Proceedings, 12th world conference on earthquake engineering. 2000. 8p.

[3] Alavi B, Krawinkler H. Effects of near-fault ground motions on frame structures. Blume center report #138. Stanford (CA); 2001. 301p.

[4] Tothong P, Cornell CA. Near-fault ground motions for seismic demand analysis. Earthquake Spectra 2007 [in press].

[5] Luco N. Probabilistic seismic demand analysis, SMRF connection fractures, and near-source effects. Stanford (CA): Dept. of Civil and Environmental Engineering, Stanford University; 2002 http://www.stanford.edu/group/rms/Thesis/.

[6] Mavroeidis GP, Papageorgiou AS. A mathematical representation of near-fault ground motions. Bulletin of the Seismological Society of America 2003;93(3):1099–131.

[7] Fu Q, Menun C. Seismic-environment-based simulation of near-fault ground motions. In: Proceedings, 13th world conference on earthquake engineering. 2004. 15p.

[8] Baker JW, Cornell CA. Vector-valued ground motion intensity measures for probabilistic seismic demand analysis. Report #150. Stanford (CA): John A. Blume Earthquake Engineering Center; 2005. 321p. http://blume.stanford.edu/Blume/Publications.htm.

[9] Abrahamson NA, Silva WJ. Empirical response spectral attenuation relations for shallow crustal earthquakes. Seismological Research Letters 1997;68(1):94–126.

[10] Somerville PG. Magnitude scaling of the near fault rupture directivity pulse. Physics of the Earth and Planetary Interiors 2003;137(1):12.

[11] Ibarra LF, Krawinkler H. Global collapse of frame structures under seismic excitations. Report #152. Stanford (CA): John A. Blume Earthquake Engineering Center; 2005. 324p. http://blume.stanford.edu/Blume/Publications.htm.

[12] Medina RA, Krawinkler H. Evaluation of drift demands for the seismic performance assessment of frames. Journal of Structural Engineering 2005;131(7):1003–13. http://link.aip.org/link/?QST/131/1003/1.

[13] FEMA. 350. Recommended seismic design criteria for new steel moment-frame buildings. SAC Joint Venture. Washington (DC): Prepared for the Federal Emergency Management Agency; 2000.

[14] Veletsos AS, Newmark NM. Effect of inelastic behavior on the response of simple systems to earthquake motions. In: Proceedings of the second world conference on earthquake engineering. 1960. p. 895–912.

[15] Veletsos AS, Newmark NM, Chelapati CV. Deformation spectra for elastic and elastoplastic systems subjected to ground shock and earthquake motions. In: Proceedings of the 3rd world conference on earthquake engineering. 1965. p. 663–80.

[16] Sasani M, Bertero V. Importance of severe pulse-type ground motions in performance-based engineering: Historical and critical review. In: Proceedings, twelfth world conference on earthquake engineering. 2000.

[17] Mavroeidis GP, Dong G, Papageorgiou AS. Near-fault ground motions, and the response of elastic and inelastic single-degree-of-freedom (sdof) systems. Earthquake Engineering & Structural Dynamics 2004;33(9): 1023–49.

[18] Fu Q. Modeling and prediction of fault-normal near-field ground motions and structural response. Ph.D. thesis. Stanford (CA): Dept. of Civil and Environmental Engineering, Stanford University; 2005.

[19] Hastie T, Tibshirani R, Friedman JH. The elements of statistical learning: Data mining, inference, and prediction. New York: Springer; 2001.

[20] Goel RK, Chopra AK. Evaluation of modal and fema pushover analyses: SAC buildings Earthquake Spectra 2004; 20(1): p. 225–54 http://link.aip.org/link/?EQS/20/225/1.

[21] Luco N, Cornell CA. Structure-specific scalar intensity measures for near-source and ordinary earthquake ground motions. Earthquake Spectra 2007;23(2):357–92.

[22] Shome N, Cornell CA. Probabilistic seismic demand analysis of nonlinear structures. RMS-35. RMS Program. Stanford (CA); 1999. 320p. http://www.stanford.edu/group/rms/.

[23] Vamvatsikos D, Cornell CA. Developing efficient scalar and vector intensity measures for IDA capacity estimation by incorporating elastic spectral shape information. Earthquake Engineering & Structural Dynamics 2005;34(13):1573–600. http://dx.doi.org/10.1002/eqe.496.

[24] Baker JW, Cornell CA. Choice of a vector of ground motion intensity measures for seismic demand hazard analysis. In: Proceedings of the 13th world conference on earthquake engineering. 2004. 15p.

[25] Neter J, Kutner MH, Nachtsheim CJ, Wasserman W. Applied linear statistical models. 4th ed. Boston: McGraw-Hill; 1996.

[26] Baker JW, Cornell CA. A vector-valued ground motion intensity measure consisting of spectral acceleration and epsilon. Earthquake Engineering & Structural Dynamics 2005;34(10):1193–217.

[27] Bazzurro P, Cornell CA. Vector-valued probabilistic seismic hazard analysis. In: 7th US national conference on earthquake engineering. 2002. 10p.

[28] Abrahamson NA. Effects of rupture directivity on probabilistic seismic hazard analysis. In: Sixth international conference on seismic zonation. 2000.

[29] Abrahamson NA. Statistical properties of peak ground accelerations recorded by the SMART 1 array. Bulletin of the Seismological Society of America 1988;78(1):26–41.

[30] Tothong P, Cornell CA, Baker JW. Probabilistic seismic hazard analysis accounting for the possibility of near-fault velocity pulses. Earthquake Spectra 2007 [in press].

[31] Bazzurro P, Cornell CA. Seismic hazard analysis of nonlinear structures I: Methodology. Journal of Structural Engineering 1994;120(11):3320–44.

[32] Stewart JP, Chiou S-J, Bray JD, Graves RW, Somerville PG, Abrahamson NA. Ground motion evaluation procedures for performance-based design. PEER 2001–09. Berkeley (CA): Pacific Earthquake Engineering Research Center, University of California at Berkeley; 2001. 229p.